Stress-Induced Phase Transition in $\mathbf{Pb(Zr_{1/2}Ti_{1/2})O_3}$

Nicholas J. Ramer,* Steven P. Lewis,* E. J. Mele†,‡ and Andrew M. Rappe*,‡

*Department of Chemistry, †Department of Physics and
‡Laboratory for Research on the Structure of Matter
University of Pennsylvania, Philadelphia, PA 19104

Abstract. We investigate, within local density functional theory, the structural phase stability of the piezoelectric material $Pb(Zr_{1/2}Ti_{1/2})O_3$ (PZT) under finite applied uniaxial stress. Previous theoretical analyses of piezoelectric properties have examined the behavior of the system near the ground-state structure. However, because some piezoelectrics can accept large ($> 1\%$) strains reversibly [J. Appl. Phys. **82**, 1804 (1997)], these crystals are clearly operating beyond their lowest-order behavior, and insight can be gained from studying piezoelectricity at finite strain. We have studied the structural properties of the (111)-PZT crystal over a range of positive and negative uniaxial strains. For each strain state, we identity two metastable structures: a tetragonal phase and a low-symmetry rhombohedral-like phase. For each phase, we determine the evolution of the magnitude and direction of polarization in the crystal as a function of applied stress. We also analyze the energetic and structural profile of the stress-induced tetragonal-to-rhombohedral phase transition. In particular, we compute the transition stress, and we identify the accompanying atomic motions in terms of larger structural motifs such as cation motion within oxygen cages and oxygen-cage tilting.

INTRODUCTION

$PbZr_xTi_{1-x}O_3$ (PZT) is an important material for use in actuator applications. The structural phase diagram of PZT and its dependence on composition and temperature have been studied experimentally [1–6] for the past forty years and more recently, theoretically [7,8] in much detail. Most PZT ceramics employed in modern solid-state devices are synthesized with a lead zirconate to lead titanate ratio that is close to the tetragonal-rhombohedral morphotropic phase boundary (approximately 50/50 batch composition). Near this boundary, PZT ceramics have high electro-mechanical coupling and low coercive fields.

Structural phase transitions in ferroelectric materials induced by hydrostatic pressure have been extensively studied experimentally [9]. For example, 95/5 PZT

has been found to depolarize completely under hydrostatic pressure around 290 MPa [10]. In addition it has been found that 56/44 PZT will undergo partial depolarization for hydrostatic pressures of 480 MPa [10]. Most theoretical studies of PZT have been limited to phenomenological models parametrized to experimentally determined composition-temperature-pressure data points [7]. These models are based on a simplified Landau-Devonshire theory [11,12] for the free energy of ferroelectric materials. Recently, a first-principles study of the hydrostatic-pressure-induced phase transition in zero-temperature $PbTiO_3$ was conducted using full-potential muffin-tin orbitals within the local density approximation [13]. It was found that at a critical pressure of 16.4 GPa, $PbTiO_3$ would undergo a tetragonal-to-cubic phase transition. The computed compressibilities and their dependence on pressure were in good agreement with available experimental data.

Because many modern piezoelectric device applications involve longitudinal or uniaxial stresses, experiments have investigated the response of piezoelectric materials under uniaxial stress [14,15]. Recently, experimental techniques have been developed and implemented to determine accurately the piezoelectric coefficients and dielectric constants of commercially-available compositions of PZT [16]. For PZT compositions near the morphotropic phase boundary, the tetragonal-rhombohedral phase transition induced by uniaxial compressive stress has recently been suggested as a possible cause of polarization reorientation in pulsed high-voltage electric fields [17].

With the advent of piezoelectric materials that can accept large strains, a microscopic understanding of these materials at finite strain has become more important. In this work, we study the effect of applying a uniaxial stress to a 50/50 PZT crystal. (We will refer to this composition as PZT for the remainder of this paper.) By examining structural phases of PZT on both sides of the morphotropic phase boundary, we elucidate the evolution of structural features (and therefore the polarization) as a function of applied stress.

METHODOLOGY

The first-principles calculations presented in this paper are performed within density functional theory [18] in the local density approximation (LDA). The single electron wave functions are expanded in a plane-wave basis using a cutoff energy of 50 Ry.

To describe the electron-nuclear interaction, optimized pseudopotentials [19] in fully separable nonlocal form [20] are used. An additional feature of our nonlocal pseudopotentials [21] is their improved transferability over a wide range of electronic configurations, obtained by judiciously exploiting the flexibility contained in the separation of the local and nonlocal parts of the pseudopotential. By designing the form of the local potential so that the pseudo-eigenvalues and all-electron eigenvalues agree at an additional charge state, it is possible to improve the transferability of the potential across the charge states lying between the original reference

TABLE 1. Computed equilibrium lattice constants for tetragonal and rhombohedral (111)–$Pb(Zr_{1/2}Ti_{1/2})O_3$ (PZT). Experimental lattice constants are given for randomly ordered PZT ceramics close to the 50-50 batch composition.

	Present	Experiment[a]		Present	Experiment[b]
Tetragonal (111)–PZT			**Rhombohedral (111)–PZT**		
c(Å)	8.199	8.279	c(Å)	8.052	8.163
c/a	1.042	1.027	$\angle(^\circ)$	89.64	89.79

[a] Ceramic **3** reference [24].
[b] Ceramic **5** reference [24].

state and this second state.

In order to obtain the high accuracy needed in examining ferroelectric phenomena, semi-core shells are in the generation of the pseudopotentials. We include as valence states the $3s$ and $3p$ for Ti and the $4s$ and $4p$ for Zr. The $5d$ shell is included for Pb. Furthermore, scalar relativistic effects are included in the generation of the Pb pseudopotential [22]. Brillouin zone integrations were approximated accurately as sums on a $4 \times 4 \times 4$ Monkhorst-Pack k-point mesh [23].

We have applied uniaxial stress along the (100) direction to two structurally distinct phases of a (111)-PZT superlattice. In the tetragonal phase, the polarization direction is (100), parallel to the applied stress. In the rhombohedral-like phase, the polarization in the unrelaxed crystal is oriented along (111), which is the stacking direction for planes of like cations. Upon structural relaxation, the polarization in the rhombohedral-like phase gains a (100) component in response to the applied stress.

Complete relaxation of both atomic positions and in-plane lattice constant were performed for a variety of fixed unit cell heights. We have neglected the shear response to uniaxial stress. We estimate that the contribution of shear to the energetics of the rhombohedral-like phase is less that 0.01 eV/unit cell. The relaxation of the in-plane lattice constants introduces a component of isotropic pressure into the analysis. However, by permitting this structural relaxation, we can more closely simulate the experimental conditions.

RESULTS

The experimental and theoretical lattice parameters are contained in Table 1. Our results agree well with experiment for both phases. The theoretical lattice constants are smaller than experiment by 1–1.5%, as is usual for calculations done with the LDA [25,26]. Figure 1 shows the equations of state (total energy as function of unit cell height) for the two phases of the (111)-PZT superlattice. We find

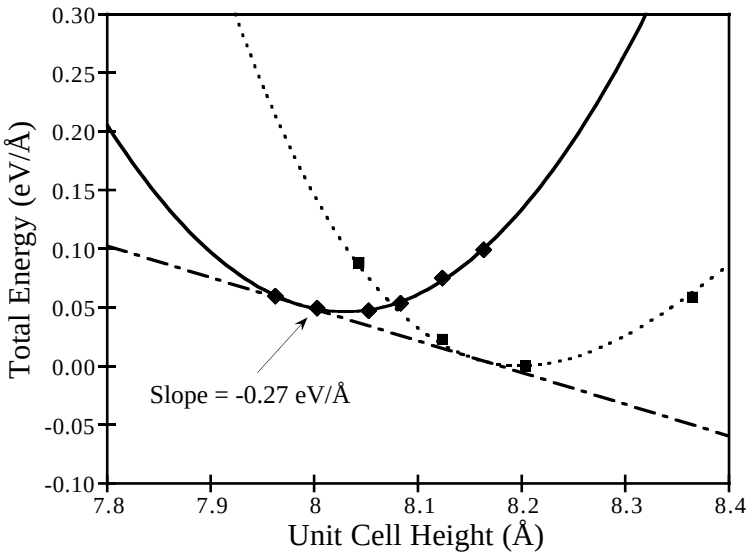

FIGURE 1. Equations of state for the tetragonal (dotted-line) and rhombohedral-like (solid-line) phases of (111)–$Pb(Zr_{1/2}Ti_{1/2})O_3$. The solid line represents the rhombohedral-like phase and the dotted line shows the tetragonal phase. The heights and energies are for a 40-atom unit cell.

that the tetragonal phase is the ground-state structure. However, under compressive stress, the rhombohedral-like phase becomes more favorable. Additionally, we find that the tetragonal phase shows significant anharmonicity versus strain, while anharmonicity is small for the rhombohedral-like phase. Specifically, we find a 13% change in the transition stress if the cubic fit shown is replaced by a quadratic fit to the data that are near the equilibrium.

In order to examine the interatomic structural motifs that characterize the two phases as a function of stress, we have plotted illustrative distances from fixed features within the unit cell. For brevity, we include only the TiO_6 octahedron response. We have omitted the ZrO_6 octahedron response because of its similarity to the TiO_6 octahedron and PbO_{12} dodecahedron response due to its complexity. In the rhombohedral-like phase, there are four crystallographically unique oxygen atoms in the TiO_6: two equatorial and two axial. In the tetragonal phase, there are three crystallographically unique oxygens: one equatorial and two axial.

In Figure 2 we have plotted the distance of the Ti atom and axial oxygens from the equatorial plane of oxygen within the TiO_6 octahedron. In the case of the rhombohedral-like phase, the equatorial plane is not constrained by symmetry to lie perpendicular to the (100). Therefore we have computed an average distance from the plane.

The width of the TiO_6 can be analyzed by computing the diagonal distance of the equatorial plane of oxygens. We have plotted this distance as a function of unit cell height for both phases in Figure 3.

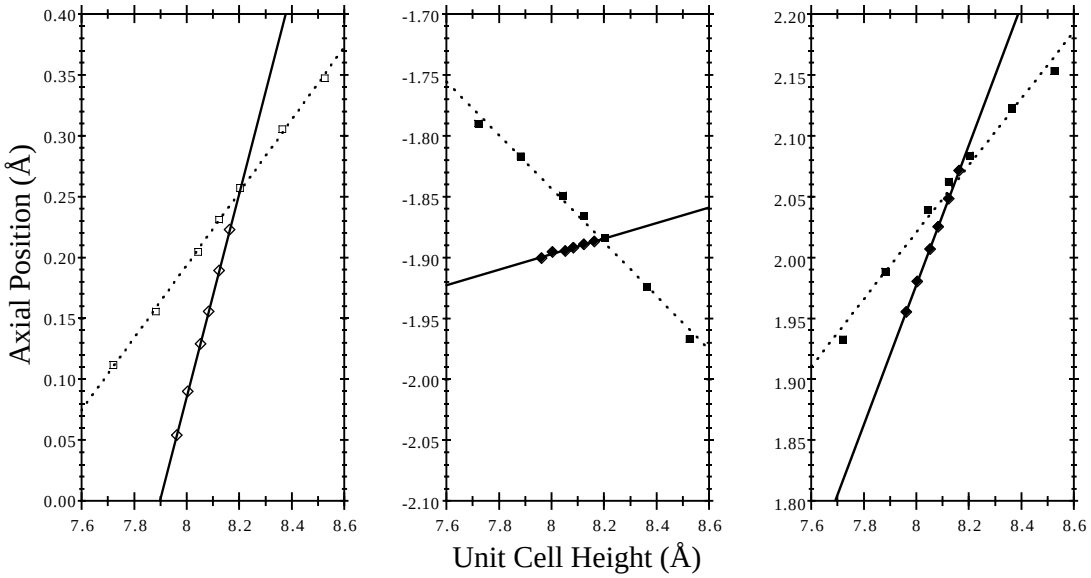

FIGURE 2. Positions relative to the equatorial oxygen plane in the TiO_6 octahedron of Ti (left) and axial O atoms (center, right) as a function of unit cell height for the tetragonal and rhombohedral-like phases of (111)–$Pb(Zr_{1/2}Ti_{1/2})O_3$. The solid lines and diamonds represent the rhombohedral-like phase, and the dotted lines and squares show the tetragonal phase.

GIBBS CONSTRUCTION

For materials under applied uniaxial force, F, we can construct a generalized enthalpy:

$$H(L) = E(L) + FL \tag{1}$$

Any structure adjusts its unit cell height, L, to minimize its enthalpy:

$$\frac{dE}{dL} = -F \tag{2}$$

At zero temperature, a phase transition occurs when two competing phases have equal enthalpy.

$$E_1 + FL_1 = E_2 + FL_2 \tag{3}$$

Rearranging (3) yields

$$-F = \frac{(E_2 - E_1)}{(L_2 - L_1)} = \left.\frac{dE_2}{dL}\right|_{L_2} = \left.\frac{dE_1}{dL}\right|_{L_1} \tag{4}$$

where the last two equalities in equation (4) come from equation (2).

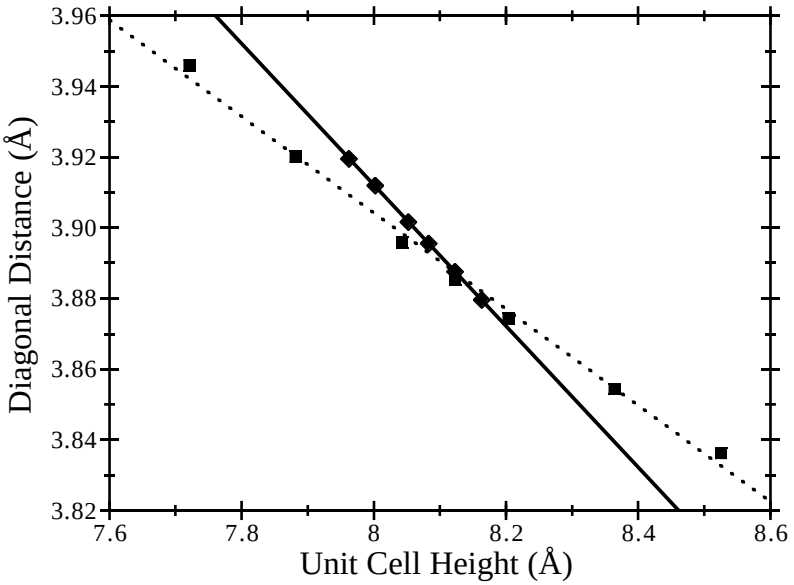

FIGURE 3. Equatorial oxygen plane diagonal distance as a function of unit cell height for the tetragonal and rhombohedral-like phases of (111)–$Pb(Zr_{1/2}Ti_{1/2})O_3$. The solid lines and diamonds represent the rhombohedral-like phase and the dotted lines and squares show the tetragonal phase.

Thus, a first-order phase transition occurs between points on the equations of state of the two phases that are connected by a common tangent line. Then, the transition stress, σ, is found via $F = \sigma A$, where A is the unit cell area, and $-F$ is the slope of the common tangent.

The line of common tangent for the PZT tetragonal and rhombohedral-like phases has been plotted in Figure 1. The slope of this line is -0.27 eV/Å. This represents the uniaxial force per conventional surface unit cell necessary to cause the phase transition. The sign of the transition force shows that compressive stress will cause a phase transition from the tetragonal phase to the rhombohedral-like. The unit cell height at the transition is 7.987Å for the rhombohedral-like phase and 8.157Å for the tetragonal phase. By examining the in-plane lattice constant relaxations, we can determine the area of the unit cell perpendicular to the direction of uniaxial stress at these transition cell heights. From this we compute the compressive transition stress to be 669 ± 6 MPa.

DISCUSSION

Anharmonicity in Tetragonal Phase

As stated above, our finite stress approach has revealed some anharmonicity in the tetragonal phase equation of state. In addition, our analysis of structural fea-

tures shows a slight nonlinearity in the B-metal/oxygen bond lengths as a function of applied stress. Also, the change in the TiO_6 equatorial size with applied stress shows a nonlinearity for the tetragonal phase (see Figure 3). These results further highlight the importance of going beyond lowest order in understanding the behavior of these materials. The origin of this anharmonicity is difficult to ascertain from the present study, and its examination is ongoing. Anharmonicity should also be found in the rhombohedral-like phase for stresses larger than those applied in the present study.

Trends in Structural Motifs

Rhombohedral-like Phase

For the uniaxial compression of the rhombohedral-like phase, we find decreasing axial distances from the equatorial plane for the Ti atom and the oxygen atom near it (see Figure 2). We find that as a compressive uniaxial stress is applied, the Ti atom moves toward the equatorial plane. The O in the same half of the octahedron as the Ti atom moves with it while the O on the other side remains nearly stationary. These motions indicate a decrease in magnitude of the (100) component of the local polarization in the TiO_6 octahedron as this phase is compressed. We have also completed an analysis of the (011) motions of the axial atoms relative to the center of the equatorial plane. These motions are negligible on the scale of the axial motions parallel to the applied stress. In response to uniaxial stress, the (100) component of polarization decreases while the other components remain intact.

Tetragonal Phase

The response of the tetragonal phase of (111)-PZT to uniaxial compression is quite different from that of the rhombohedral-like phase. Upon compression we find that all the axial atoms relax towards the equatorial oxygen plane (see Figure 2). In fact, the Ti and both axial oxygens atoms move at nearly the same rate. This response of all three axial atoms is in sharp contrast with the rhombohedral-like phase which showed larger response in the Ti and the O in the same half of the octahedron, but negligible response of the other axial O atom. The magnitude of response (both axial and equatorial) is smaller in the tetragonal phase. This is because to the (100) compression is parallel to the direction of polarization for the tetragonal phase.

CONCLUSIONS

In this density functional study, we have made the first prediction of a uniaxial stress-induced phase transition from first-principles methods. We have exam-

ined the tetragonal and rhombohedral-like phases of the (111)-$Pb(Zr_{1/2}Ti_{1/2})O_3$ crystal under (100) uniaxial stress. Characterization of the two metastable structural phases emphasizes the importance of strain coupling to polarization, since the simplest Landau theory of polarization, in which strain is neglected, does not permit more than one metastable structure [27]. We have found that a compressive stress of 669 MPa will cause a tetragonal-to-rhombohedral phase transition in (111)-$Pb(Zr_{1/2}Ti_{1/2})O_3$. Our calculations use LDA predictions of lattice parameters throughout, and this may affect the predicted transition stress. Quantitative comparison of the computed transition stress with experiment is difficult due to the absence of experimental studies on this phase transition. Most modern studies [28,29] of uniaxial stress on PZT materials focus on donor-doped (soft) materials that undergo polarization switching at lower stresses than undoped PZT. The work by Schäufele presents the closest comparison to the current study. In their work, neodymium-doped soft PZT ($Pb_{0.97}Nd_{0.02}(Zr_{1/2}Ti_{1/2})O_3$) is subjected to uniaxial compression. For this material, 50-200 MPa was needed to completely reorient the polarization of the material under various applied electric fields. Since our calculation does not incorporate donor doping or structural disorder, our transition stress must therefore be considered an upper limit to transition stresses of real PZT materials.

It is thought that for many perovskite materials, the *magnitude* of polarization remains nearly constant as stress is applied, and that the major contribution to the piezoelectricity is from *rotation* of the polarization vector. In order to assess the effect of uniaxial stress on (111)-PZT, we have analyzed relevant atomic distances in the TiO_6 octahedron in order to isolate distortions that would contribute to certain components of the polarization. For the rhombohedral-like phase, we find a reduction of the (100) component of polarization upon uniaxial compression, but almost no change in the polarization in other directions. This polarization response is inconsistent with a pure rotation model. In the tetragonal phase, we find atomic motions parallel to the direction of uniaxial compression. These motions give rise to a decrease in the magnitude of polarization.

Finite stress analyses done in conjunction with spontaneous polarization studies will aid the understanding of lead zirconate-titanate ceramics and other piezoelectric materials.

ACKNOWLEDGMENTS

The authors would like to thank Karin Rabe and David Vanderbilt for valuable discussions during this project. This work was supported by the Laboratory for Research on the Structure of Matter and the Research Foundation at the University of Pennsylvania as well as NSF grants DMR 93-13047 and DMR 97-02514 and the Petroleum Research Fund of the American Chemical Society (Grant No. 32007-G5). Computational support was provided by the National Center for Supercomputing Applications and the San Diego Supercomputer Center.

REFERENCES

1. Shirane, G., Suzuki, K., and Takeda, A., *J. Phys. Soc. Japan* **7**, 12 (1952).
2. Shirane, G., and Suzuki, K., *J. Phys. Soc. Japan* **7**, 333 (1952).
3. Shirane, G., and Takeda, A., *J. Phys. Soc. Japan* **7**, 5 (1952).
4. Clarke, R., and Glazer, A. M., *Ferroelectrics* **12**, 207 (1976).
5. Multani, M. S., Gokarn, S. G., Vijayaraghavan, R., and Palkar, V. R., *Ferroelectrics* **37**, 652 (1981).
6. Zhang, H., Uusimäki, A., Leppävuori, S., and Karjalainen, P., *J. Appl. Phys.* **76**, 4292 (1994).
7. Porat, Y., Imry, Y., Aharony, A., and Bransky, I., *Ferroelectrics* **37**, 591 (1981).
8. Haun, M. J., Furman, E., McKinstry, H. A., and Cross, L. E., *Ferroelectrics* **99**, 27 (1989).
9. Hegenbarth, E., *Ferroelectrics* **22**, 79 (1978).
10. Data provided by Gulton Industries, Inc., cited in Mock, W., and Holt, W. H., *J. Appl. Phys.* **49**, 5846 (1978).
11. Devonshire, A. F., *Phil. Mag.* **40**, 1040 (1949).
12. Devonshire, A. F., *Phil. Mag.* **42**, 1065 (1951).
13. Mryasov, O. N., Novikov, D. L., and Freeman, A. J., *Ferroelectrics* **164**, 279 (1995).
14. Berlincourt, D., and Krueger, H., *J. Appl. Phys.* **30**, 1804 (1959).
15. Cao, H., and Evans, A. G., *J. Am. Ceram. Soc.* **76**, 890 (1993).
16. Zhang, Q. M., Zhao, J., Uchino, K., and Zheng, J., *J. Mater. Res.* **12**, 226 (1997).
17. Sadykov, S. A., Bondarenko, E. G., and Agalarov, A. S., *Tech. Phys.* **38**, 965 (1993).
18. Payne, M. C., Teter, M. P., Allan, D. C., Arias, T. A., and Joannopoulos, J. D., *Rev. Mod. Phys.* **64**, 1045 (1992), and references therein.
19. Rappe, A. M., Rabe, K. M., Kaxiras, E., and Joannopoulos, J. D., *Phys. Rev. B* **41**, 1227 (1990).
20. Kleinman, L., and Bylander, D. M., *Phys. Rev. Lett.* **48**, 1425 (1982).
21. Ramer, N. J., and Rappe, A. M., *Phys. Rev. B*, submitted.
22. Koelling, D. D., and Harmon, B. N., *J. Phys. C* **10**, 3107 (1977).
23. Monkhorst, H. J., and Pack, J. D., *Phys. Rev. B* **13**, 5188 (1976).
24. Jaffe, B., Roth, R. S., and Marzullo, S., *J. Res. Nat. Bur. Stand.* **55**, 239 (1955).
25. Ramer, N. J., Mele, E. J., and Rappe, A. M., *Ferroelectrics*, in press, (1997).
26. Saghi-Szabo, G., and Cohen, R. E., *Ferroelectrics*, in press, (1997).
27. Vanderbilt, D. H., private communication, (1998).
28. Lynch, C. S., *Acta Mater.* **44**, 4137 (1996).
29. Schäufele, A. B., and Härdtl, K. H., *J. Am. Ceram. Soc* **79**, 2637 (1996).